

STRUCTURE OF MATTER
AND QUANTUM CHEMISTRY

Quantum-Chemical Calculations on the Stability and Mobility of Vacancies in Graphene

A. A. Kuzubov^{a,b,c}, Yu. E. Anan'eva^a, A. S. Fedorov^{a,b}, F. N. Tomilin^{a,b}, and P. O. Krasnov^{b,c}

^aSiberian Federal University, Krasnoyarsk, 660041 Russia

^bKirensky Institute of Physics, Siberian Branch, Russian Academy of Sciences, Krasnoyarsk, 660036 Russia

^cSiberian State Technological University, Krasnoyarsk, 660049 Russia

e-mail: alex_xx@rambler.ru

Received April 19, 2011

Abstract—Thermodynamic stabilities of mono- and bivacancies in graphene for deformed and non-deformed lattices are estimated by means of quantum-chemical calculations. Monovacancy hopping constants are evaluated in dependence on the applied uniaxial deformations.

Keywords: graphene, defects, quantum-chemical simulation, deformations.

DOI: 10.1134/S0036024412070126

INTRODUCTION

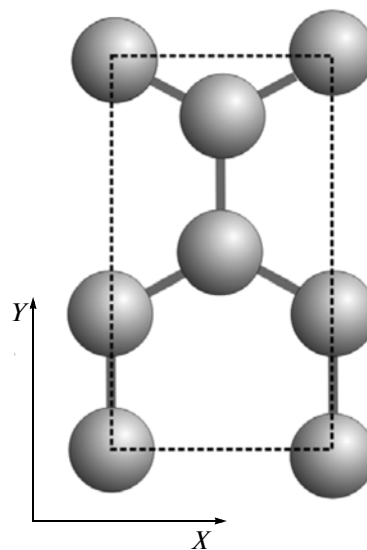
Graphene is now considered to be a most promising material. A great many investigations have been devoted to the properties of this unique material [1–4] and various methods for synthesizing it have been suggested [5–8]. Graphene, like all real crystals, has defects that seriously affect its properties. These can appear in the stages of growth or purification as a result of ionic bombardment and so on. Crystal lattice defects obviously affect the electronic and mechanical properties of graphene.

Defects of different types can be present in graphene layers: Stone–Wales defects, mono- and bivacancies, and adatoms of carbon and other elements. The presence of these defects has been proved experimentally [9–12]. If methods for synthesizing graphene sheets on different substrates are used, stresses must be present in the prepared carbon structures due to the difference between the lattice parameters for the structure itself and for the substrate [7]. Such stresses in the material can change its properties, influencing the stability and mobility of defects. There are many papers devoted to analyzing the structure and mechanisms of the formation of defects in graphene layers [9, 11]. In virtually none of them, however, is the dynamics of vacancies considered for deformed layers, i.e., layers with stress.

The aim of this work is a theoretical investigation of the dependences of stability and mobility of mono- and bivacancies on the degree of lattice deformation and temperature.

CALCULATION METHODS

Calculations were performed within the density functional theory (DFT) formalism using the VASP (Vienna ab Initio Simulation Package) program [13–15]. Pseudopotentials (Vanderbilt potentials [16]) and a plane-wave basis expansion of the wave functions are used in this program for quantum-chemical calculations. The calculations were performed with allowance for periodic conditions. A 7×5 supercell of rectangular graphene cells corresponding to $17.196 \times 21.274 \text{ \AA}$ (referred to below as X and Y lattice vectors) (figure)



Rectangular cell of graphene.

was used to exclude the mutual influence of vacancies in one plane.

In order to exclude interaction between graphene plates, a vacuum space was of 10 Å was inserted between them. The cutting energy of plane waves used in our calculations was 286.7 eV. The calculations were performed by dividing the reciprocal lattice space into a $3 \times 3 \times 1$ network using the Monkhorst Pack method [17]. The self-coordinated geometry optimization procedure was performed with a precision of 1×10^{-3} eV. The nudged elastic band method [18] was used to find the transition state and potential barriers for the hopping of vacancies in graphene.

The defect-free graphene structure and the structures with mono- and bivalencies containing 140, 139, and 138 carbon atoms, respectively, was initially simulated. To discover the effect of uniaxial deformation on the stability and mobility of defects in a graphene layer, calculations were performed with alternating changes in the lattice translation vectors in the X and Y directions. Defect-free and defect structures were considered with decremented and incremented (by 2 and 5%) translation vectors along each of the directions. Geometry was optimized such that pressure was present only along the pre-selected direction.

Formation energies of vacancies was determined according to the formula

$$E_v = E_{\text{def.str}} - E_{\text{ndef.str}} + E_{\text{at C}}, \quad (1)$$

where E_v is the formation energies of mono- and bivalencies, $E_{\text{def.str}}$ is the energy of a structure with a vacancy, $E_{\text{ndef.str}}$ is the energy of a vacancy-free structure, and $E_{\text{at C}}$ is the energy of carbon atom in the graphene phase.

To analyze the mobility of monovacancies in dependence on the degree of deformation, we calculated the rate constants for the hopping of vacancies. The rate constants for the graphene plane were calculated within the transition state theory with allowance for the zero point energy E_0 of atom vibration using the Arrhenius formula:

$$k = A e^{-\frac{E_b}{kT}}, \quad (2)$$

where E_b is the potential barrier height, defined as the difference between the energies of the transition complex and the equilibrium state. The energy was calculated for the transition state with allowance for the zero point vibration energy,

$$E_0^\# = \sum_{i=1}^{3N-7} \frac{\hbar \nu_i^\#}{2},$$

while in the case of the equilibrium state,

$$E_0 = \sum_{i=1}^{3N-6} \frac{\hbar \nu_i}{2},$$

Table 1. Dependence of the energies of defects on deformation

Deformation	E_{mv} , eV	E_{bv} , eV
Without deformation	7.808	7.302
Compression X 5%	5.379	2.386
Compression X 2%	6.962	5.587
Stretching X 2%	7.681	9.131
Stretching along X by 5%	7.373	10.136
Compression along Y by 5%	6.552	8.465
Compression along Y by 2%	7.417	7.894
Stretching along Y by 2%	7.361	6.860
Stretching along Y by 5%	6.838	6.223

Note: E_{mv} and E_{bv} are the energies of formation for mono- and bivalencies, respectively.

where N is the number of displaced atoms. The preexponential factor A was calculated using the Vineyard formula,

$$A = \frac{kT}{\hbar} \left[\prod_{i=1}^{3N-6} \left(1 - e^{-\frac{\hbar \nu_i}{kT}} \right) \right] / \left[\prod_{i=1}^{3N-7} \left(1 - e^{-\frac{\hbar \nu_i^\#}{kT}} \right) \right]$$

where T is temperature, and ν and $\nu^\#$ are vibration frequencies for the optimum and transition state, respectively.

RESULTS AND DISCUSSION

The dependence of formation energies (E_v) of mono- and bivalencies on the applied deformation was obtained from the data obtained after optimizing the structures' geometry (Table 1).

It was found that bivalencies are more thermodynamically advantageous than monovacancies in a nondeformed graphene structure.

The pattern of defect stabilities, however, changes upon the deformation of the investigated structures. It was established that compressive deformation along the X direction (or tensile deformation along the Y direction) lowers the energy of bivalency formation, increasing their stability. In this case, bivalencies are more stable than in nondeformed structures. Under the same conditions, their stability is higher than that of monovacancies.

Any deformation of a structure with monovacancies enhances their stability relative to a nondeformed structure. Nothing similar was observed in the case of bivalencies.

Applying a uniaxial tensile deformation along the X direction (or compressive deformation along Y direction) results in the stabilization of monovacancies with respect to bivalencies. Under these conditions, the formation energy of bivalencies in deformed struc-

Table 2. Temperature dependence of the hopping constant (s^{-1}) of vacancies

Deformation (monovacancy)	$T = 77$ K	$T = 298$ K	$T = 873$ K
Without deformation	1.80×10^{-58}	3.40×10^{-6}	5.68×10^6
Compression along X by 5%	7.44×10^{-106}	8.91×10^{-20}	0.21×10^3
Compression along X by 2%	4.09×10^{-60}	3.92×10^{-6}	1.08×10^7
Stretching along X by 2%	1.43×10^{-48}	2.70×10^{-3}	5.32×10^7
Stretching along X by 5%	1.91×10^{-22}	7.43×10^1	2.61×10^9
Compression along Y by 5%	3.87×10^7	2.05×10^{11}	1.51×10^{12}
Compression along Y by 2%	5.06×10^{-23}	7.08×10^3	8.70×10^9
Stretching along Y by 2%	6.49×10^{-82}	6.86×10^{-12}	4.83×10^4
Stretching along Y by 5%	9.72×10^{-195}	3.57×10^{-41}	1.13×10^5

tures is higher (i.e., their stability is lower) than in nondeformed structures.

The concentrations of mono- and bivacancies in the graphene structure thus likely depend on the direction of the stress that arises due to interaction with the substrate.

The kinetic parameters of the process are calculated below. Potential barrier energies (E_b) for the motion of vacancies along the Y direction were calculated using the nudged elastic band method. It should be noted that the Y direction of deformation is parallel to the motion of a vacancy, while the X direction is perpendicular. For nondeformed structures containing mono- and bivacancies, the barrier value was 1.07 and 6.02 eV, respectively. The rather high value of the potential barrier energy for structures with bivacancies testifies to the low-probability mobility of these defects. It can be seen from the calculations that the potential barrier value depends on the degree of structural deformation and the type of defect.

It is known that graphene can exist over a wide range of temperatures. Calculations of the rate constants for the hopping of vacancies were therefore performed at 77, 298, and 873 K (Table 2).

It can be seen from Table 2 that deformation can lead to both an increase and a decrease in defect mobility. The mobility of a monovacancy is increased upon compression of the structure along the direction parallel to the motion of the vacancy (Y) or its stretching along the perpendicular direction (X). A reduction in the mobility of a monovacancy is observed upon tensile deformation along the Y direction or compressive deformation along the X direction.

An increase in mobility due to deformation leads to the random migration of a monovacancy. It should not, however, result in the recombination of single monovacancies into a bivacancy, since the thermodynamic stability of bivacancies is considerably reduced

and that of monovacancies is enhanced by deformations facilitating single vacancy migration.

The mobility of monovacancies increases with temperature (Table 2), as is the case for most processes.

REFERENCES

1. K. S. Novoselov, *Science* **306** (5696), 666 (2004).
2. K. S. Novoselov, *Proc. Nat. Acad. Sci. USA* **102**, 10451 (2005).
3. S. V. Morozov, K. S. Novoselov, M. I. Katsnelson, et al., *Phys. Rev. Lett.* **100**, 156 (2008).
4. A. Balandin, S. Ghosh, and W. Bao, *Nano Lett.* **8**, 902 (2008).
5. S. Zhengzong, Y. Zheng, E. Beitler, et al., *Nature* **468**, 549 (2010).
6. A. K. Geim and K. S. Novoselov, *Nature Mater.* **6**, 183 (2007).
7. D. Usachov, A. M. Dobrotvorskii, and A. Varykhalov, *Phys. Rev. B* **78**, 1–8 (2008).
8. S. Yu. Davydov, A. A. Lebedev, and N. Yu. Smirnova, *Solid State Phys.* **51**, 481 (2009).
9. F. Banhart, J. Kotakoski, and A. V. Krashenninnikov, *ACS Nano* **5** (1), 26 (2011).
10. M. H. Gass, U. Bangert, and A. L. Bleloch, *Nature Nanotechnol.* **3**, 265 (2008).
11. A. Hashimoto, *Nature* **430**, 870 (2004).
12. C. Jannic, C. Kisielowski, R. Erni, et al., *Nano Lett.* **8**, 3582 (2008).
13. G. Kresse and J. Hafner, *Phys. Rev.* **47**, 558 (1993).
14. G. Kresse and J. Hafner, *Phys. Rev.* **48**, 13115 (1993).
15. G. Kresse and J. Hafner, *Phys. Rev.* **49**, 14251 (1994).
16. D. Vanderbilt, *Phys. Rev.* **41**, 7892 (1990).
17. H. J. Monkhorst and J. D. Pack, *Phys. Rev.* **13**, 5188 (1976).
18. G. Henkelman, B. P. Uberuagaand, and H. Jonsson, *J. Chem. Phys.* **113**, 9901 (2000).